Advances in Nano Research, *Vol. 17, No.5 (2024) 435-444*
https://doi.org/10.12989/anr.2024.17.5.435

Dynamic response with fraction laws: Eigen solution of clamped-simply supported rotating shell

Emad Ghandourah[1], Muzamal Hussain*[2], Mohamed A. Khadimallah[3], Hamdi Ayed[4], Monzoor Ahmad[5], Lahcen Azrar[6] and Abir Mouldi[7]

[1]*Department of Nuclear Engineering, Faculty of Engineering, King Abdulaziz University, Jeddah, Saudi Arabia*
[2]*Department of Mathematics, University of Sahiwal, Sahiwal, 57000, Pakistan*
[3]*Department of Civil Engineering, College of Engineering in Al-Kharj, Prince Sattam Bin Abdulaziz University, Al-Kharj, 11942, Saudi Arabia*
[4]*Department of Civil Engineering, College of Engineering, King Khalid University, Abha - 61421, Saudi Arabia*
[5]*Department of Mathematics, University of Azad Jammu and Kashmir, Muzaffarabad, 1300, Azad Kashmir, Pakistan*
[6]*Department of Applied Mathematics and Informatics, ENSAM, Mohammed V University of Rabat, Morocco*
[7]*Department of Industrial Engineering, College of Engineering, King Khalid University, Abha - 61421, Saudi Arabia*

(*Received February 3, 2022, Revised September 23, 2024, Accepted October 2, 2024*)

Abstract. The shell problem in this work is modeled as a rotating cylindrical shell with three distinct volume fraction rules. There is a connection between polynomial, exponential, and trigonometric fraction laws and the governing equations for shell motion. The fundamental natural frequency is examined for several parameters, including height-radius and length-to-diameter ratios. The resulting backward and forward frequencies rise with rising height-to-radius ratios, whereas frequencies decrease with increasing length-to-radius ratios. Furthermore, as the angular speed increases, the forward and reverse frequencies decrease and increase, respectively. By using MATLAB coding, the eigen solutions of the frequency equation have been found. The findings for the clamped simply supported condition have been taken out of this numerical procedure in order to examine the properties of shell vibration. The generated results provide evidence for the applicability of the current shell model and are also supported by previously published material.

Keywords: clamped- simply supported fraction laws; frequency response; rotating speed

1. Introduction

Numerous domains, including charge detectors, electronics, communication, composite materials, bio-technology, the environment, energy storage, chemistry, and optics, are possible applications for cylindrical shells. The employment of cylindrical shells in pressure vessels, silos, core-barrels of pressure water reaction, and chimney design is widespread in practical applications. In theoretical and applied mechanics, vibration investigation is an important field of study (Yuan *et al*. 2024, Wang *et al*. 2023). Applications for shells in engineering science and technology are numerous. Their applications can be found, for instance, in the fields of nuclear, mechanical, electrical, aerodynamics, missile technology, spline-rotor systems, ship structure, and aerodynamics (Zhang and Ma 2022).

The functionally graded materials are composed of multiple types of materials, and their physical characteristics differ on different surfaces. These surfaces differ mechanically and physically in a regular manner from one another, giving them a dual physical appearance. One of these surfaces has a high degree of heat resistance, while the other may maintain significant dynamic perseverance. Each of these materials has interchangeable inner and outer surfaces, and they all have rather different physical characteristics and sandwich structure (Suresh and Mortensen 1997, Koizumi 1997, Liu *et al*. 2022). These materials are arranged according to different methods, and dynamic elements like plates, beams, and shells use them. -Additionally, they have been seen in ship pipeline systems, spacecraft, nuclear reactors, missile technologies, and valve spool structures (Li *et al*. 2024, Zhang *et al*. 2024).

Based on the particle swarm approach, Shi *et al*. (2024) looked into the optimum design for couple bearing surface texture. In 2021, Li and colleagues presented the scaling-Basis Chirplet Transform. The frequencies of fluid-filled composite cylindrical shells were found by Sharma *et al*. (1998). They used trigonometric functions to estimate the axial modal deformations. The vibrations of infinitely long spinning, thin, isotropic cylindrical shells were studied by Di Taranto and Lessen in 1964. Pre-stress influence on buckling and vibration features of rotating cylindrical shells was analyzed by Padovan (1975). A fluid-submerged cylindrical shells (CS) was analytically investigated by Goncalves and Batista (1987). Sharma (1974) used the Rayleigh-Ritz formulation to examine the vibration frequencies of a circular cylinder and compared his findings with a few experimental ones. Research on isotropic long rotating cylindrical shells, including the impact of coriolis effects on their traveling modes, was carried out by Srinivasan and Lauterbach in 1971. The frequency response of fluid-filled cylindrical shells (CSs) was examined by

*Corresponding author, Ph.D.,
E-mail: muzamal45@gmail.com;
muzamalhussain@uosahiwal.edu.pk

ISSN: 2287-237X (Print), 2287-2388 (Online)

Chung *et al*. (1981), who also provided an analysis of their experimental and analytical research. Generalized end conditions were used by Penzes and Kraus (1972) to examine the vibrations of rotating cylindrical shells. The approximation approach and calculation process were required, the analysis of rotating shells was limited to a few exceptional circumstances. Advanced computers have completely transformed shell vibration analysis with their sophisticated numerical approaches. Rotating cylindrical shell vibrations were studied by Fox and Hardie (1985). For the shell motion equations, they employed Flugge's shell theory. Donnell's shallow-shell model with the quiescent, dense, inviscid, and incompressible fluid was utilized by Amabili *et al*. (1999). Additionally, the impact of the shell's internal and external sides is investigated in relation to the dense fluid. Internally, the shell was thought to be entirely filled, but the fluid outside the shell was thought to be an unbounded domain that extended in all directions. Several scholars (Saito and Endo 1996, Wang *et al*. 1994, Chen *et al*. 1993) employed the shell motion equations for rotating cylindrical shells. The vibrations of spinning composite and sandwich cylindrical shells were studied by Lam and Loy (1994). They compared the vibration frequencies of revolving composite cylindrical shells and assessed the outcomes using various shell theories. Using sigmoid law distribution and the hygrothermal impact, Pankaj *et al*. (2019) investigated the functionally graded material. Aspect ratio frequency spectra have been illustrated with respect to different edge situations. Vibration frequencies and modes of rotating composite composite shafts were examined by Li and Lam (1998) in relation to edge circumstances. Different approaches were employed by a number of researchers to investigate frequency analysis (Golabchi *et al*. 2018, Lal and Markad 2018, Mousavi *et al*. 2019a, Loghman *et al*. 2017, Sayin and Calayir, 2015, Zheng *et al*. 2021, Faleh *et al*. 2018, Fenjan *et al*. 2020a, b, Abdulrazzaq *et al*. 2020, Ahmed *et al*. 2021, Kong *et al*. 2024, Chen *et al*. 2024, Khadimallah *et al*. 2020a, b, Hussain 2022, Hussain *et al*. 2024, Hussain and Naeem, 2019, Muzamal 2022, Qazaq *et al*. 2022).

The control and automation shield machine was created by Qin *et al*. (2024a, b). Sun *et al*. (2025) and Chai *et al*. (2024) looked into vibration measurement using a semantic segmentation network and an algorithm. In 1968, Sewall and Naumann examined the vibration analysis of computer systems using both analytical and experimental techniques. Linear stiffeners were used to reinforce the shells. The vibrations of rotating cylindrical shells with limited length were examined by Zohar and Aboudi (1973), and the vibration of the shell was derived using a matrix approach. In their 2007 study, Najafizadeh and Isvandzibaei established their angular deformation theory of higher order by using ring supports to CSs for vibration analysis along the tangential direction. The effects of constituent volume fractions and shell configurations on the shell vibrations were ascertained by using the angular deformation in shell equations. The FG material properties were gradually altered. Cylindrical shell vibration was studied by Ergin and Temarel (2002). The shells were horizontally oriented, filled with fluid, and submerged in it. Eltaher *et al*. (2019), Ebrahimi *et al*. (2019), Safaei *et al*. (2019), Shahsavari *et al*. (2019), Benmansour *et al*. (2019), Miaofen *et al*. (2023), Wang *et al*. (2014). Researchers have recently employed many techniques for nonlinear modeling.

The current study looks at the frequency characteristics of spinning FG cylindrical shells. Furthermore, almost little is known about or assumed about the angular frequency characteristics of shells with various geometrical parameters (ratios of thickness to radius and length to radius). Materials that are functionally graded are thought to be organized. The clamped-simply (C-S) boundary condition applied to the ends of a cylindrical shell, along with its reference surface, length, radius, and thickness characteristics, are used to explain the shell's dynamic behavior. Vibration causes a stationary wave to be created when a static cylindrical shell moves. Furthermore, as the angular speed increases, the forward and reverse frequencies decrease and increase, respectively. The resulted presented here are produced by the MATLAB computer program.

2. Effective material properties

Functionally graded materials work best in extremely heated systems. Their fabric qualities depend on the temperature under these circumstances. According to Touloukian (1973) definition, if χ denotes a fabric attribute and is dependent upon the absolute temperature T (K), then

$$\chi = \chi_0(\chi_{-1}T^{-1} + \chi_1 T + \chi_2 T^2 + \chi_3 T^3) \tag{1}$$

The thermal coefficients are defined here by χ_0, χ_{-1}, χ_1, χ_2 and χ_3 and the temperature (K) is expressed in Kelvin degrees. The following are the fabric qualities that result from a FGM:

$$\chi = \sum_{i=1}^{\dagger} \chi_i V_{f_i} \tag{2}$$

The number of functionally graded ingredient fabrics is † wherever χ_i denotes the fabric property and the volume fraction V_{fi} of the i^{th} FGM in that order. The outcome of adding the volume fractions of these component materials is one that is

$$\sum_{i=1}^{\dagger} V_{f_i} = 1 \tag{3}$$

3. Volume fraction laws

Three volume fraction rules are examined in the vibrations of rotating FG circular cylindrical shells: polynomial, exponential, and trigonometric. In the direction of the shell radius, these principles regulate the functionally graded material composition.

$$\text{Law-I: Polynomial Law } V_f = \left(\frac{z}{h} + \frac{1}{2}\right)^{\Gamma} \tag{4}$$

Law-II: Exponential Law $V_f = 1 - e^{-\left(\frac{2}{h}+\frac{1}{2}\right)^{\Gamma}}$ (5)

Law-III: Trigonometric Law $V_{f1} = cos^2\left[\left(\frac{2}{h}+\frac{1}{2}\right)^{\Gamma}\right]$ (6)

$$V_{f2} = sin^2\left[\left(\frac{2}{h}+\frac{1}{2}\right)^{\Gamma}\right] \quad (7)$$

The term V_f is designated as total volume fraction of FG-CS, respectively. The power exponent is denoted as Γ and h for thickness and z is the coordinate.

Functionally graded materials are created when two or more materials, such as Nickel and Stainless steel, are mixed together. Depending on the compositional order, these shells are divided into two categories. Their configuration has a significant impact on how FG-CSs form. The constituent ingredients of FG are arranged as Type-I and Type-II, but in reverse order. At temperature 300K, the material properties for FG-CS are:E, υ, ρ for Stainless steel are $2.07788 \times 10^{11}\frac{N}{m^2}$, 0.317756 and $8166\frac{Kg}{m^3}$ and Nickel are $2.05098 \times 10^{11}\frac{N}{m^2}$, 0.3100, and 8900 $\frac{Kg}{m^3}$.

So the Young's modulus E_{fgm}, Poisson ratio v_{fgm} and mass density ρ_{fgm} for three different laws are defined as:

Law-II: FGM Polynomial Law

$$E = (E_1 - E_2)\left(\frac{Z}{h}+\frac{1}{2}\right)^{\Gamma} + E_2 \quad (8)$$

$$v = (v_1 - v_2)\left(\frac{Z}{h}+\frac{1}{2}\right)^{\Gamma} + v_2 \quad (9)$$

$$\rho = (\rho_1 - \rho_2)\left(\frac{Z}{h}+\frac{1}{2}\right)^{\Gamma} + \rho_2 \quad (10)$$

Law-II: FGM Exponential Law

$$E = (E_1 - E_2)\left(1 - a^{-\left(\frac{Z}{h}+\frac{1}{2}\right)^{\Gamma}}\right) + E_2 \quad (11)$$

$$v = (v_1 - v_2)\left(1 - a^{-\left(\frac{Z}{h}+\frac{1}{2}\right)^{\Gamma}}\right) + v_2 \quad (12)$$

$$\rho = (\rho_1 - \rho_2)\left(1 - a^{-\left(\frac{Z}{h}+\frac{1}{2}\right)^{\Gamma}}\right) + \rho_2 \quad (13)$$

Law-III: FGM Trigonometric Law

$$E = (E_1 - E_2)\, sin^2\left[\left(\frac{Z}{h}+\frac{1}{2}\right)^{\Gamma}\right] + E_2 \quad (14)$$

$$v = (v_1 - v_2)\, sin^2\left[\left(\frac{Z}{h}+\frac{1}{2}\right)^{\Gamma}\right] + v_2 \quad (15)$$

$$\rho = (\rho_1 - \rho_2)\, sin^2\left[\left(\frac{Z}{h}+\frac{1}{2}\right)^{\Gamma}\right] + \rho_2 \quad (16)$$

When $z = -\frac{h}{2}$ is substituted in the expressions (8) to (16), $E = E_2$, $\nu = \nu_2$ and $\rho = \rho_2$ which are material properties of Type-I and when substitution $z = \frac{h}{2}$ is made in the above expressions, $E = E_1$, $\nu = \nu_1$ and $\rho = \rho_1$ for a Type-II. These substitutions demonstrate the continuous transition of the fabric Type-I qualities at the shell's internal surface to Type-II properties at the shell external surface, which is connected to its mid surface. Given that the ratio of radius to thickness in a FG-CS consisting of two materials is more than twenty, any suitable thin shell theory can be applied to study the vibration characteristics of this heterogeneous shell.

4. Theoretical formulations

As illustrated in Fig. 1, the z - co-ordinates are obtained in their radial directions, and the x, θ -co-ordinates are considered to be along the longitudinal and circumferential directions, respectively.

Here, ρ_t stands for density and is written as

$$\rho_t = \int_{\frac{-h}{2}}^{\frac{h}{2}} \rho\, dz \quad (17)$$

where, A_{ij}, B_{ij}, and D_{ij} respectively, indicate the stiffness condition of the FG-shell and are explained as:

In case of isotropic, Q_{ij} is reduced stiffness

$$Q_{11} = Q_{22} = \frac{E}{1-\nu^2} \quad (18)$$

$$\left.\begin{aligned} A_{ij} &= \int_{\frac{-h}{2}}^{\frac{h}{2}} Q_{ij} dz \\ B_{ij} &= \int_{\frac{-h}{2}}^{\frac{h}{2}} z Q_{ij} dz \\ D_{ij} &= \int_{\frac{-h}{2}}^{\frac{h}{2}} z^2 Q_{ij} dz \end{aligned}\right\} \quad (19)$$

For isotropic materials, Q_{ij} is the reduced stiffness with the conjunction of E and $\upsilon$is expressed as follows:

$$Q_{22} = \frac{E}{1-v^2} \quad (20)$$

$$Q_{12} = \frac{vE}{1-v^2} \quad (21)$$

$$Q_{66} = \frac{E}{2(1+v)} \quad (22)$$

Making use of the rotating cylinder differential operator notation from sander shell theory as

$$\text{ñ}_{11}\, u + \text{ñ}_{12}\, v + \text{ñ}_{13}\, w = R^2 \rho_t \frac{\partial^2 v}{\partial t^2} \quad (23)$$

$$\bar{\mathfrak{m}}_{21}\, u + \bar{\mathfrak{m}}_{22}\, v + \bar{\mathfrak{m}}_{23} = R^2 \rho_t \left(\frac{\partial^2 v}{\partial t^2} + £ \frac{\partial w}{\partial t} - £^2 v \right) \quad (24)$$

$$\bar{\mathfrak{m}}_{31}\, u + \bar{\mathfrak{m}}_{32}\, v + \bar{\mathfrak{m}}_{33}\, w = R^2 \rho_t \left(\frac{\partial^2 w}{\partial t^2} - £ \frac{\partial v}{\partial t} - £^2 w \right) \quad (25)$$

where

$$\bar{\mathfrak{m}}_{11} = A_{11} \frac{\partial^2}{\partial x^2} + \left(\frac{A_{66}}{R^2} + \rho_t £^2 \frac{\partial^2}{\partial \theta^2} \right).$$

$$\bar{\mathfrak{m}}_{12} = \frac{(A_{12} + A_{66})}{R} \frac{\partial^2}{\partial x \partial \theta} + \frac{(B_{12} + 2B_{66})}{R^2} \frac{\partial^2}{\partial x \partial \theta}$$

$$\bar{\mathfrak{m}}_{13} = \left(\frac{A_{12}}{R} - \rho_t £^2 R \right) \frac{\partial}{\partial x} - B_{11} \frac{\partial^3}{\partial x^3} - \frac{(B_{12} + 2B_{66})}{R^2} \frac{\partial^3}{\partial x \partial \theta^2}$$

$$\bar{\mathfrak{m}}_{21} = \left(\frac{A_{12} + A_{66}}{R} + \frac{B_{12} + B_{66}}{R^2} + \rho_t £^2 R \right) \frac{\partial^2}{\partial x \partial \theta}$$

$$\bar{\mathfrak{m}}_{22} = \left(A_{66} + \frac{3B_{66}}{R} + \frac{2D_{66}}{R^2} \right) \frac{\partial^2}{\partial x^2} + \left(\frac{A_{22}}{R^2} + \frac{2B_{22}}{R^3} + \frac{D_{22}}{R^4} \right) \frac{\partial^2}{\partial \theta^2} + \rho_t £^2$$

$$\bar{\mathfrak{m}}_{23} = \left(\frac{A_{22}}{R^2} + \frac{B_{22}}{R^3} \right) \frac{\partial}{\partial \theta} - \left(\frac{B_{22}}{R^3} + \frac{D_{22}}{R^4} \right) \frac{\partial^3}{\partial \theta^3} - \left(\frac{B_{12} + 2B_{66}}{R} + \frac{D_{12} + 2D_{66}}{R^2} \right) \frac{\partial^3}{\partial x^2 \partial \theta} - 2\rho_t £ \frac{\partial}{\partial t}$$

$$\bar{\mathfrak{m}}_{31} = -\frac{A_{12}}{R} \frac{\partial}{\partial x} + B_{11} \frac{\partial^3}{\partial x^3} + \left(\frac{B_{12} + 2B_{66}}{R^2} \right) \frac{\partial^3}{\partial x \partial \theta^2}$$

$$\bar{\mathfrak{m}}_{32} = -\left(\frac{A_{22}}{R^2} + \frac{B_{22}}{R^3} + \rho_t £^2 \right) \frac{\partial}{\partial \theta} + \left(\frac{B_{22}}{R^3} + \frac{D_{22}}{R^4} \right) \frac{\partial^3}{\partial \theta^3} + \left(\frac{B_{12} + 2B_{66}}{R} + \frac{D_{12} + 4D_{66}}{R^2} \right) \frac{\partial^3}{\partial x^2 \partial \theta} + 2\rho_t £ \frac{\partial}{\partial t}$$

$$\bar{\mathfrak{m}}_{33} = -\frac{A_{22}}{R^2} + \rho_t £^2 + \frac{2B_{12}}{R} \frac{\partial^2}{\partial x^2} + \left(\frac{2B_{22}}{R^3} + \rho_t £^2 \right) \frac{\partial^2}{\partial \theta^2} - D_{11} \frac{\partial^4}{\partial x^4} - 2 \left(\frac{D_{12} + 2D_{66}}{R^2} \right) \frac{\partial^4}{\partial x^2 \partial \theta^2} - \frac{D_{22}}{R^4} \frac{\partial^4}{\partial \theta^4}$$

The displacement components are represented as follows in the first order shear deformation theory:

$$U(x, \theta, t) = \alpha_m\, U(x)\, Sin\,(n\theta + \omega t) \quad (26)$$

$$V(x, \theta, t) = \beta_m\, V(x)\, Cos\,(n\theta + \omega t) \quad (27)$$

$$W(x, \theta, t) = \gamma_m\, W(x)\, Sin\,(n\theta + \omega t) \quad (28)$$

where *U*, *V*, and *W* are the unknown functions that, in turn, represent the corresponding deformations in the transverse, tangential, and longitudinal directions. The vibration amplitudes in the *x*, *θ*, and *z* directions are represented by the coefficients α_m, β_m and γ_m respectively. The angular frequency of the shell is described by *ω* (rad/sec), while *n* indicates the circumferential wavenumber. The axial wave number is indicated by the subscript *m*. For different boundary conditions, the exponents of the complex exponential functions that define the functions *U*, *V*, and *W* are related to the axial wave number k_m.

i.e., $U(x)=V(x)=W(x)=e^{-ik_m x}$

The modal displacement functions (26)-(28) are then substituted into the governing Eqs. (23)-(25) once the value of *U(x) = V(x) = W(x)* has been entered into them. One can obtain algebraic expressions in their full form:

$$\begin{Bmatrix} -k_m^2 A_{11} - n^2 \left(\frac{A_{66}}{R^2} + \rho_t £^2 \right) + \rho_t \omega^2 \end{Bmatrix} U + \begin{Bmatrix} -ink_m \left(\frac{A_{12} + A_{66}}{R} + \frac{B_{12} + 2B_{66}}{R^2} \right) \end{Bmatrix} V + \begin{Bmatrix} -ik_m^3 B_{11} - ik_m \left(\frac{A_{12}}{R} - \rho_t £^2 R \right) \\ -in^2 k_m \left(\frac{B_{12} + 2B_{66}}{R^2} \right) \end{Bmatrix} W = 0 \quad (29)$$

$$\begin{Bmatrix} ink_m \left(\frac{A_{12} + A_{66}}{R} + \frac{B_{12} + B_{66}}{R^2} + \rho_t £^2 R \right) \end{Bmatrix} U + \begin{Bmatrix} -k_m^2 \left(A_{66} + \frac{3B_{66}}{R} + \frac{2D_{66}}{R^2} \right) \\ -n^2 \left(\frac{A_{22}}{R^2} + \frac{2B_{22}}{R^3} + \frac{D_{22}}{R^4} \right) + \rho_t £^2 \rho_t \omega^2 \end{Bmatrix} V + \begin{Bmatrix} -n \left(\frac{A_{22}}{R^2} + \frac{B_{22}}{R^3} \right) - n^3 \left(\frac{B_{22}}{R^3} + \frac{D_{22}}{R^4} \right) \\ -nk_m^2 \left(\frac{B_{12} + 2B_{66}}{R} + \frac{D_{12} + 2D_{66}}{R^2} \right) + 2£\rho_t \omega \end{Bmatrix} W = 0 \quad (30)$$

$$\begin{Bmatrix} ik_m \frac{A_{12}}{R} + ik_m^3 B_{11} + in^2 k_m \left(\frac{B_{12} + 2B_{66}}{R^2} \right) \end{Bmatrix} \alpha_m + \begin{Bmatrix} -n \left(\frac{A_{22}}{R^2} + \frac{B_{22}}{R^3} + \rho_t £^2 \right) - n^3 \left(\frac{B_{22}}{R^3} + \frac{D_{22}}{R^4} \right) \\ -nk_m^2 \left(\frac{B_{12} + 2B_{66}}{R} + \frac{D_{12} + 4D_{66}}{R^2} \right) + 2£\rho_t \omega \end{Bmatrix} \beta_m + \begin{Bmatrix} -\frac{A_{22}}{R^2} + \rho_t £^2 - k_m^2 \frac{2B_{12}}{R} - n^2 \left(\frac{2B_{22}}{R^3} + \rho_t £^2 \right) \\ -k_m^4 D_{11} - 2n^2 k_m^2 \left(\frac{D_{12} + 2D_{66}}{R^2} \right) - n^4 \frac{D_{22}}{R^4} + \rho_t \omega^2 \end{Bmatrix} \gamma_m = 0 \quad (16)$$

The word arrangement for the eigenvalue form is framed as

$$\{ \tilde{\Delta}_1 \omega^2 + \tilde{\Delta}_2 \omega + \tilde{\Delta}_3 \}[x] = 0 \quad (32)$$

Here $\tilde{\Delta}_1$, $\tilde{\Delta}_2$, $\tilde{\Delta}_3$ signify order three square matrices. The shell parameters are implicated by the matrix entries $\tilde{\Delta}_3$.

Six eigenvalues make up the solution, hence out of these values, the smallest absolute real value is selected. Eigen frequency divides into two components during the rotation of a cylindrical shell: the positive and negative rotating sections. When the shell rotates, the standing wave splits into forward and backward waves based on the direction of rotation. When the shell vibrates, these two frequencies are comparable, but they are static. According to the frequency values, the forward frequencies are lower than the backward wave frequencies.

5. Results and discussion

For the current model's validity and effectiveness, some frequency work is done. A comparison between the simply supported condition and wave number *n* = 1~5 is presented in Table 1 (Loy *et al*. 1997). A comparison of the analytical frequencies of shell for = 2, 3 is shown in Table 2 (Ahmad and Naeem 2009). Table 2 presents a good agreement between Ahmad and Naeem (2009) and the simply supported shell ends conditions of natural frequencies (Hz)

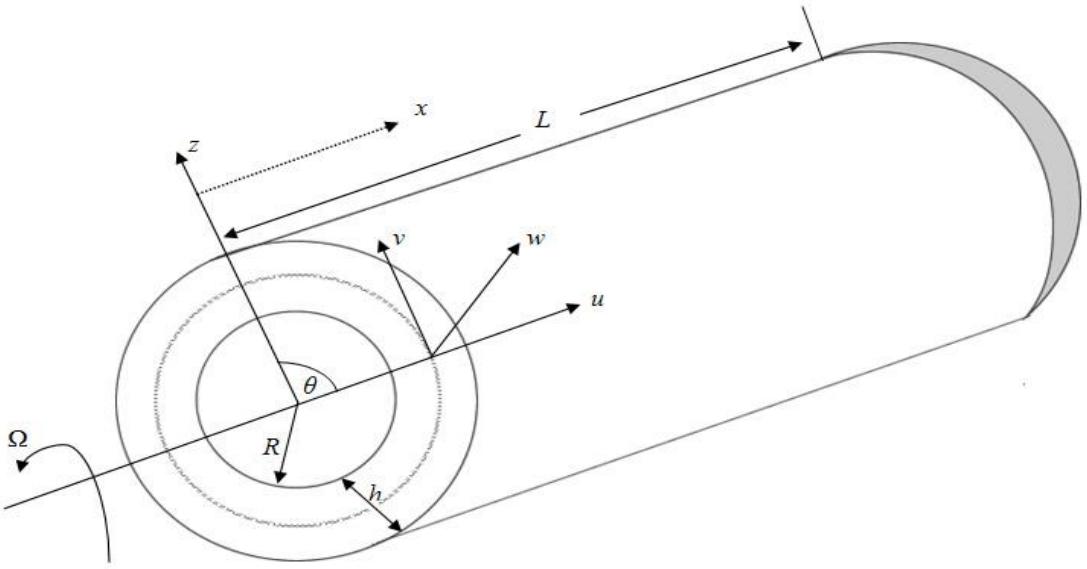

Fig. 1. Labeling the rotating CS's geometry

Table 1 The frequency of a cylindrical shell edge condition that is simply supported and functionally graded (Loy *et al*. 1997)

n	m	Loy *et al*. (1997)	Present
	1	2045.3	2046.4
	2	5636.5	5637.2
2	3	8934.9	8933.4
	4	11406.7	11407.8
	5	13252.7	13253.0

Table 2 The frequency of a cylindrical shell edge condition with a simply supported functionally graded structure (Ahmad and Naeem 2009)

n	m	Ahmad and Naeem (2009)	Present
	1	2043.77	2046.4
	2	5635.37	5637.1
2	3	8932.46	8933.4
	4	11407.4	11407.7
	5	13253.1	13253.0
	1	2195.05	2199.0
	2	4035.55	4041.2
3	3	6614.63	6619.2
	4	9121.10	9124.1
	5	11358.91	11360.8

for circumferential wave number n = 2, 3. The axial form m varies from 1 to 5. Enhancing the value of m leads to an increase in the natural frequency. Table 2 lists the geometrical and material parameters (ν, E, ρ), (L, R, h). Table 3 demonstrates the mathematical values that Naeem and Sharma (2000) looked into. Natural frequency values nowadays are considerably nearer and somewhat higher than those of (Naeem and Sharma, 2000). The Type-I and

Table 3 According to Naeem and Sharma (2000), the frequency of an S-S functionally graded cylindrical shell edge conditions vs n

n	Naeem and Sharma (2000)	Present
4	287.59	288.49
5	201.85	202.33
6	166.59	166.56
7	166.22	165.63
8	189.29	188.15
9	226.88	225.26
10	274.09	271.99
11	328.64	326.03
12	389.49	386.37
13	456.21	452.53
14	528.57	524.28
15	606.45	601.51

Table 4 For C-S edge conditions, the frequency of non-rotating FG-CS against n for Type I: ($m = 1, {}^{h}/_{R} = 0.003$, ${}^{L}/_{R} = 15$)

n	Polynomial	Exponential
1	22.428	22.416
2	7.6512	7.6463
3	6.3897	6.3786
4	10.482	10.462
5	16.535	16.463
6	24.184	24.152
7	33.258	33.188
8	43.739	43.698
9	55.621	55.528
10	68.903	68.881

Table 5 For C-S edge conditions, the frequency of non-rotating FG-CS against n for Type II: ($m = 1, {}^{h}/_{R} = 0.002$, ${}^{L}/_{R} = 20$, $\Gamma = 0.7$)

n	Polynomial	Exponential	Trigonometric
1	13.151	13.162	13.175
2	4.4521	4.4586	4.4607
3	4.1249	4.2272	4.2327
4	6.9928	7.2913	7.3245
5	11.173	11.206	11.291
6	16.359	16.385	16.399
7	22.225	22.320	22.541
8	29.602	29.690	29.719
9	37.647	37.685	37.691
10	46.639	46.669	46.689

Table 6 For C-S edge conditions, the frequency of rotating FG-CS against n for Type I: ($m = 1$, ${}^{h}/_{R} = 0.01$, ${}^{L}/_{R} = 10$, £ $= 1$, $\Gamma = 30$)

n	Polynomial		Exponential		Trigonometric	
	Backward	Forward	Backward	Forward	Backward	Forward
1	47.523	47.224	47.431	47.152	47.326	47.118
2	17.758	17.504	17.515	17.360	17.154	17.099
3	19.633	19.441	19.467	19.276	19.125	18.994
4	34.501	34.351	34.301	34.251	34.189	34.039
5	55.204	55.082	54.941	54.718	54.586	54.364
6	80.758	80.654	80.500	80.396	80.233	80.129
7	111.01	110.93	110.98	110.47	110.32	110.11
8	145.95	145.87	145.84	147.72	145.66	145.09
9	185.56	185.49	185.37	185.25	185.19	185.03
10	229.83	229.77	229.71	229.65	229.51	229.38

Table 7 For C-S edge conditions, the frequency of rotating FG-CS against n for Type II: ($m = 1, {}^{h}/_{R} = 0.002$, ${}^{L}/_{R} = 20$, £ $= 1$, $\Gamma = 0.5$)

n	Polynomial		Exponential		Trigonometric	
	Backward	Forward	Backward	Forward	Backward	Forward
1	13.260	12.945	13.283	12.955	13.306	12.965
2	4.5693	4.3147	4.5774	4.3157	4.5784	4.3167
3	4.2263	4.0353	4.2336	4.0363	4.2346	4.0373
4	7.0670	6.9171	7.0785	6.9181	7.0808	6.9192
5	11.219	11.097	11.238	11.107	11.261	11.117
6	16.377	16.274	16.404	16.286	16.427	16.296
7	22.494	22.405	22.530	22.415	22.553	22.430
8	29.560	29.481	29.607	29.491	29.630	29.503
9	37.571	37.501	37.632	37.511	37.655	37.521
10	46.465	46.528	46.602	46.538	46.625	46.549

Type-II frequency fluctuations with clamped simply condition (C-S) end conditions are plotted against n in Tables 4 and 5. Three rules of volume fractions limit the material work of the shell: (I), (II), and (III). It demonstrates that the frequency derived from the polynomial law is greater than the frequency derived from the other two laws. It demonstrates that the frequency as defined by the trigonometric law is greater than the frequency as determined by the other two laws. For the circumferential wave number n, the natural frequencies (Hz) of a rotating functionally graded cylindrical shell design are displayed in Tables 6 and 7. The volume fraction rules, also known as the polynomial (Law-I), exponential (Law-II), and trigonometric (Law-III), have been used to establish the variance in frequencies. As their circumferential wave number (n) increases, so do the forward and backward frequencies.

The forward and backward frequencies for the polynomial volume law are higher than those for the other two laws. The natural frequencies (Hz) of a rotating cylindrical shell with functionally graded plotted against the angular speeds, £, are shown in Tables 8 and 9. These

Table 8 Rotating FG-CS frequency vs angular speed £ for C-S edge situations in Type I: ($m = 1$, ${}^{h}/_{R} = 0.03$, ${}^{L}/_{R} = 10$, $n = 2$, $\Gamma = 30$)

£	Polynomial		Exponential		Trigonometric	
	Backward	Forward	Backward	Forward	Backward	Forward
0	11.633	11.583	11.403	11.301	11.163	11.101
1	11.939	11.244	11.677	11.993	11.407	10.783
2	12.179	10.999	11.912	10.732	11.632	10.522
3	12.4163	10.7833	12.123	10.521	11.823	10.271
4	12.6479	10.586	12.341	10.311	12.041	10.059
5	12.8783	10.373	12.571	10.1091	12.221	9.8411
6	13.099	10.1733	12.771	9.9051	12.391	9.6411
7	13.331	9.9433	12.993	9.6833	12.599	9.4332
8	13.5683	9.7532	13.173	9.5001	12.798	9.2293
9	13.7937	9.5609	13.395	9.3211	12.985	9.0651

Table 9 Rotating FG-CS frequency vs angular speed £ for C-S edge situations in Type II: ($m = 1$, ${}^{h}/_{R} = 0.03$, ${}^{L}/_{R} = 10$, $n = 2$, $\Gamma = 30$)

£	Polynomial		Exponential		Trigonometric	
	Backward	Forward	Backward	Forward	Backward	Forward
0	11.163	11.102	11.402	11.302	11.624	11.582
1	11.407	11.782	12.678	11.992	11.932	11.243
2	11.632	10.523	11.913	10.731	12.178	10.998
3	11.821	10.272	12.122	10.522	12.414	10.7834
4	12.042	10.057	12.342	10.313	12.646	10.587
5	12.222	9.842	12.5714	10.1092	12.877	10.361
6	12.393	9.6421	12.775	9.9054	13.098	10.132
7	12.595	9.4332	12.992	9.6832	13.321	9.9434
8	12.799	9.2293	13.176	9.5006	13.567	9.752
9	12.985	9.0653	13.395	9.3212	13.794	9.5608

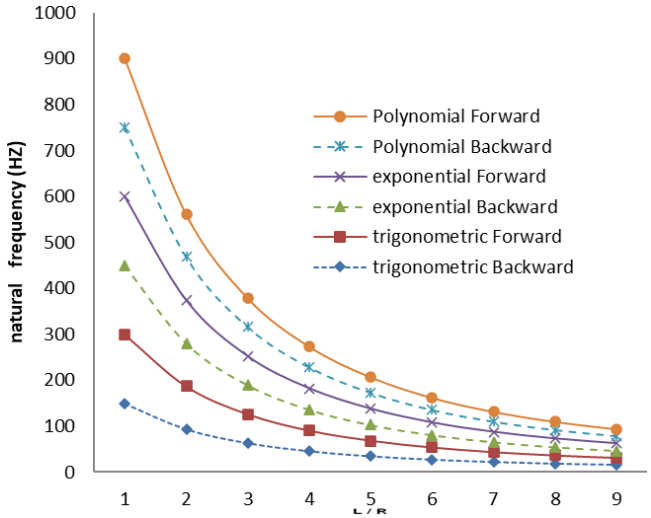

Fig. 2 The frequency of rotating FG-CS for C-S edge conditions versus L/R for Type I: ($m = 1, h/R = 0.01, \Gamma = 0.5,\ n = 2,\ £ = 3$)

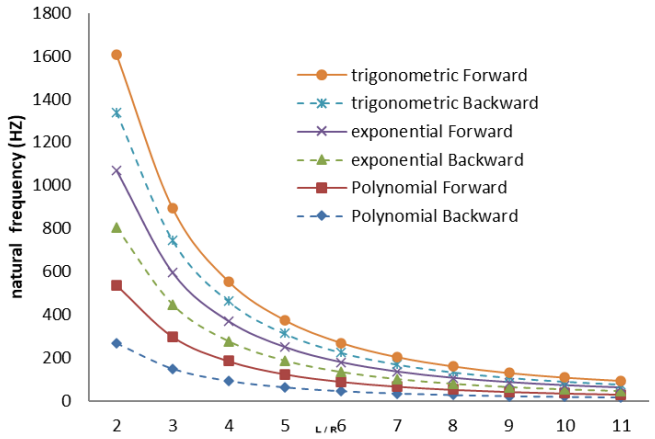

Fig. 3 The frequency of rotating FG-CS for C-S edge conditions versus L/R for Type II: ($m = 1,\ h/R = 0.01, \Gamma = 0.7,\ n = 2, £ = 3$)

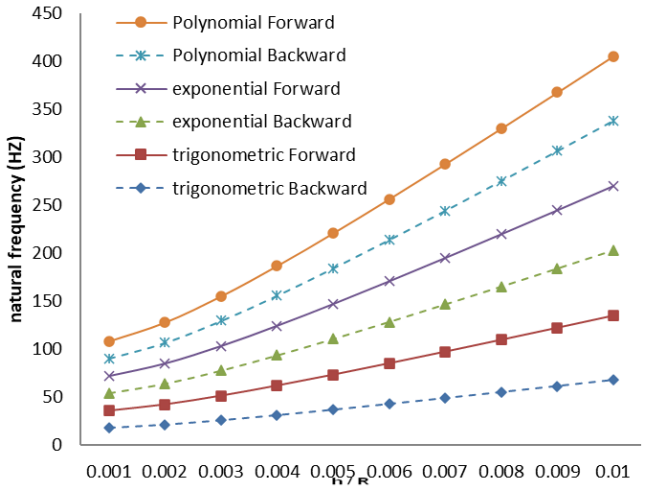

Fig. 4 The frequency of rotating FG-CS for C-S edge conditions versus h/R for Type I: ($m = 1, L/R = 10$, $N = 1,\ n = 2, £ = 3$)

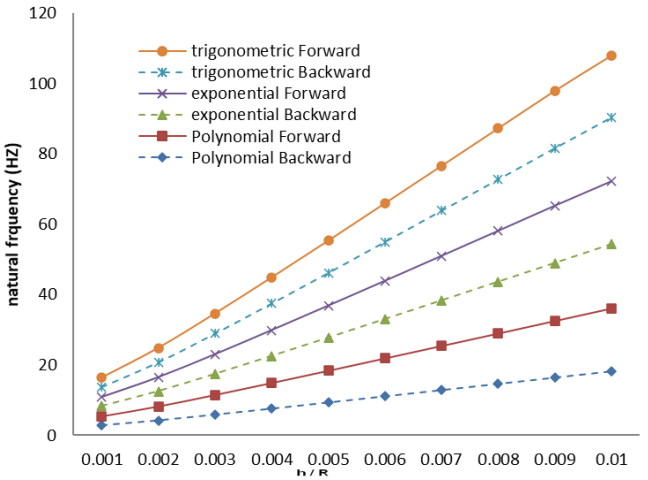

Fig. 5 The frequency of rotating FG-CS for C-S edge conditions versus h/R for Type II: ($m = 1, L/R = 20$, $N = 0.5,\ n = 3, £ = 1$)

findings were derived using the polynomial, exponential, and trigonometric volume fraction laws for the circumferential wave, n = 2. As the angular speed increases, the forward and reverse frequencies rise. The forward and backward frequencies for the polynomial volume law are higher than those for the other two laws. A rotating functionally graded cylindrical shell is sketched for natural frequencies (Hz) vs *L/R* for Type-I in Fig. 2. For every rule, the forward and reverse frequencies (Hz) decrease as *L/R* increases. The natural frequencies (Hz) of a rotating cylindrical shell type with functional graded rotation are plotted against *L/R* for Type-II in Figure 3. For all three volume fraction laws, the forward and backward frequencies (Hz) decrease as *L/R* increases. Regarding how the laws affect frequency variation, the forward and backward frequencies are higher than the frequencies that correspond to the other two laws. The forward and backward frequencies for the trigonometric volume law are greater than those for the polynomial and exponential laws. The natural frequencies (Hz) of a rotating functionally graded cylindrical shell for Type-I and Type-II are plotted versus the *h/R* in Figs. 4 and 5. For all three volume fraction laws, the forward and reverse frequencies (Hz) increase as *h/R* increases. However, both forward and backward frequencies related with the laws have bigger frequency changes than those connected with the other two laws. The forward and backward frequencies for the polynomial volume law are higher than those for the trigonometric and exponential laws. The frequencies of Type-II are higher than Type-I in Figs. 2-5.

6. Conclusions

Three volume fraction laws- polynomial, exponential, and trigonometric are investigated in the theoretical investigation of the vibration investigation of rotating cylindrical shells. In the direction of the shell radius, these principles regulate the functionally graded material

composition. Controlled from two or more materials are functionally graded materials. Typically, a cylindrical shell is formed from functionally graded material that is composed of two constituent materials. The shell structure of the current shell problem is made of Nickel and Stainless steel. Type I and Type II cylindrical shell arrangements are approved by switching the constituent material order from the inner and outer side. This creates two types of functionally graded cylindrical shells. The volume fraction law governs the fabric composition of a functionally graded material in the direction of shell thickness. Frequency values alter as the power law exponent varies. The impact of this investigation is being studied to prevent more issues. This process can adjust the axial wave number to accommodate any boundary condition. However, for the sake of simplicity, numerical results for rotating cylindrical shells with clamped simply supported have been investigated. These results show that the shell frequency is split into two halves, one associated with the forward wave and the other with the backward wave. The value of the backward frequency is found to be slightly higher than the forward frequency. The impact of laws governing volume fraction on shell frequencies has been investigated. A volume fraction laws forward and backward frequency curves are higher than those of two other volume fraction laws. The analysis of vibration characteristics of rotating FGM cylindrical shells with ring supports for different volume fraction laws can be done using an extension of this work.

Acknowledgement

The authors extend their appreciation to the Deanship of Research and Graduate Studies at King Khalid University for funding this work through Large Research Project under grant number RGP2/210/45.

References

Abdulrazzaq, M.A., Fenjan, R.M., Ahmed, R.A. and Faleh, N.M. (2020), "Thermal buckling of nonlocal clamped exponentially graded plate according to a secant function based refined theory", *Steel Compos. Struct*, **35**(1), 147-157. https://doi.org/10.12989/scs.2020.35.1.147

Ahmad, M. and Naeem, M.N. (2009), "Vibration characteristics of rotating FGM circular cylindrical shell using wave propagation method", *Eur. J. Sci. Res.*, **36**(2), 184-235. https://doi.org/10.1007/s00707-009-0141-z

Ahmed, R.A., Khalaf, B.S., Raheef, K.M., Fenjan, R.M. and Faleh, N.M. (2021), "Investigating dynamic response of nonlocal functionally graded porous piezoelectric plates in thermal environment", *Steel Compos. Struct.*, **40**(2), 243-254. https://doi.org/10.12989/scs.2021.40.2.243

AlSaleh, R.J. and Fuggini, C. (2020), "Combining GPS and accelerometers' records to capture torsional response of cylindrical tower", *Smart Struct. Syst.*, **25**(1), 111. https://doi.org/10.12989/sss.2020.25.1.111.

Amabili, M., Pellicano, F. and Païdoussis, M.P. (1998), "Nonlinear vibrations of simply supported, circular cylindrical shells, coupled to quiescent fluid", *J. Fluids Struct.*, **12**(7), 883-918. https://doi.org/10.1006/jfls.1998.0173

Arani, A.G., Kolahchi, R. and Esmailpour, M. (2016), "Nonlinear vibration analysis of piezoelectric plates reinforced with carbon nanotubes using DQM", *Smart Struct Syst*, **18**, 787-800. http://doi.org/10.12989/sss.2016.18.4.787

Arefi, M. and Zenkour, A.M. (2017), "Nonlinear and linear thermo-elastic analyses of a functionally graded spherical shell using the Lagrange strain tensor", *Smart Struct Syst*, **19**, 33-38. https://doi.org/10.12989/sss.2017.19.1.033

Arshad, S.H., Naeem, M.N., Sultana, N., Iqbal, Z. and Shah, A.G. (2011), "Effects of exponential volume fraction law on the natural frequencies of FGM cylindrical shells under various boundary conditions", *Arch Appl Mech*, **81**, 999-1016. https://doi.org/10.1007/s00419-010-0460-5

Benmansour, D.L., Kaci, A., Bousahla, A.A., Heireche, H., Tounsi, A., Alwabli, A.S., Alhebshi, A.M., Al-ghmady, K. and Mahmoud, S.R. (2019), "The nano scale bending and dynamic properties of isolated protein microtubules based on modified strain gradient theory", *Adv. Nano Res.*, **7**(6), 443. https://doi.org/10.12989/anr.2019.7.6.443

Boussoula, A., Boucham, B., Bourada, M., Bourada, F., Tounsi, A., Bousahla, A.A. and Tounsi, A. (2019), "A simple nth-order shear deformation theory for thermomechanical bending analysis of different configurations of FG sandwich plates", *Smart Struct. Syst.*, **25**(2), 197-218. https://doi.org/10.12989/sss.2020.25.2.197

Chai, S., Wang, S., Liu, C., Liu, X., Liu, T. and Yang, R. (2024), "A visual measurement algorithm for vibration displacement of rotating body using semantic segmentation network", *Expert Syst. Appl.*, **237**, 121306. https://doi.org/10.1016/j.eswa.2023.121306

Chen, R., Zhao, B., Xin, Q., Niu, X., Xie, Z., Lu, X. and Zou, D. (2024), "Analysis of transient lubrication and wear coupling behaviors considering thermal effect and journal misalignment for main bearings under dynamic load", *Wear*, **554-555**, 205478. https://doi.org/10.1016/j.wear.2024.205478

Chen, Y., Zhao, H.B. and Shin, Z.P. (1993), "Vibration of high speed rotating shells with calculation for cylindrical shells", *J. Sound Vib.*, **160**(1), 137-160. https://doi.org/10.1006/jsvi.1993.1010

Chung, H., Turula, P. Mulcahy, T.M. and Jendrzejczyk, J.A. (1981), "Analysis of cylindrical shell vibrating in a cylindrical fluid region", *Nucl. Eng. Des.*, **63**(1), 109-1012. https://doi.org/10.1016/0029-5493(81)90020-0.

Di Taranto, R.A. and Lessen, M. (1964), "Coriolis acceleration effect on the vibration of rotating thin-walled circular cylinder", *Trans. ASME J. Appl. Mech.*, **31**, 700-701. https://doi.org/10.1115/1.3629733

Ebrahimi, F., Dabbagh, A., Rabczuk, T. and Tornabene, F. (2019), "Analysis of propagation characteristics of elastic waves in heterogeneous nanobeams employing a new two-step porosity-dependent homogenization scheme", *Adv. Nano Res.*, **7**(2), 135. https://doi.org/10.12989/anr.2019.7.2.135

Eltaher, M.A., Almalki, T.A., Ahmed, K.I. and Almitani, K.H. (2019), "Characterization and behaviors of single walled carbon nanotube by equivalent-continuum mechanics approach", *Adv. Nano Res.*, **7**(1), 39. https://doi.org/10.12989/anr.2019.7.1.039

Ergin, A. and Temarel, P. (2002), "Free vibration of a partially liquid-filled and submerged, horizontal cylindrical shell", *Sound Vib.*, **254**(5), 951-965. https://doi.org/10.1006/jsvi.2001.4139

Faleh, N.M., Ahmed, R.A. and Fenjan, R.M. (2018), "On vibrations of porous FG nanoshells", *Int. J. Eng. Sci.*, **133**, 1-14. https://doi.org/10.1016/j.ijengsci.2018.08.00

Fenjan, R.M., Faleh, N.M. and Ridha, A.A. (2020a), "Strain gradient based static stability analysis of composite crystalline shell structures having porosities", *Steel Compos. Struct.*, **36**(6), 631-642. https://doi.org/10.12989/scs.2020.36.6.631

Fenjan, R.M., Moustafa, N.M. and Faleh, N.M. (2020b), "Scale-

dependent thermal vibration analysis of FG beams having porosities based on DQM", *Adv. Nano Res.*, **8**(4), 283-292. https://doi.org/10.12989/anr.2020.8.4.283

Fox, C.H.J. and Hardie, D.J.W. (1985), "Harmonic response of rotating cylindrical shell", *J. Sound Vib.*, **101**, 495. https://doi.org/10.1016/S0022-460X(85)80067-5

Ghosh, A, Miyamoto, Y, Reimanis, I, and Lannutti, J.J. (1997), "Functionally graded materials, manufacture, properties and applications", *Ceram. Transact. AM Ceram Soc*, **76**(71-89).

Golabchi, Hadi, Reza Kolahchi, and Mahmood Rabani Bidgoli, (2018), "Vibration and instability analysis of pipes reinforced by SiO_2 nanoparticles considering agglomeration effects", *Comput. Concr.*, **21**(4), 431-440. https://doi.org/10.12989/cac.2018.21.4.431

Hussain, M. (2022), "Controlling of ring based structure of rotating FG shell: Frequency distribution", *Adv. Concr. Constr.*, **14**(1), 35-43. https://doi.org/10.12989/acc.2022.14.1.035

Hussain, M. (2024), *Small-scale Computational Vibration of Carbon Nanotubes: Composite Structure*, CRC Press.

Hussain, M. and Naeem, M.N. (2019), "Effects of ring supports on vibration of armchair and zigzag FGM rotating carbon nanotubes using Galerkin's method", *Compos. Part B Eng.*, **163**, 548-561. https://doi.org/10.1016/j.compositesb.2018.12.144

Khadimallah, M.A., Hussain, M. and Harbaoui, I. (2020b), "Application of Kelvin's theory for structural assessment of FG rotating cylindrical shell: Vibration control", *Adv. Concr. Constr.*, **10**(6), 499-507. https://doi.org/10.12989/acc.2020.10.6.499

Khadimallah, M.A., Hussain, M., Khedher, K.M., Naeem, M.N. and Tounsi, A. (2020a), "Backward and forward rotating of FG ring support cylindrical shells", *Steel Compos. Struct.*, **37**(2), 137-150. https://doi.org/10.12989/scs.2020.37.2.137

Koizumi, M. (1997), "FGM activities in Japan", *Compos. Part B Eng.*, **28**(1-2), 1-4. https://doi.org/10.1016/S1359-8368(96)00016-9

Kong, W., Fu, T. and Rabczuk, T. (2024), "Improvement of broadband low-frequency sound absorption and energy absorbing of arched curve Helmholtz resonator with negative Poisson's ratio", *Appl. Acoust.*, **221**, 110011. https://doi.org/10.1016/j.apacoust.2024.110011

Krommer, M., Vetyukova, Y. and Staudigl, E. (2016), "Nonlinear modelling and analysis of thin piezoelectric plates: buckling and post-buckling behavior", *Smart Struct. Syst.*, **18**(1), 155-181. https://doi.org/10.12989/sss.2016.18.1.155

Lal, A. and Markad, K. (2018), "Deflection and stress behaviour of multi-walled carbon nanotube reinforced laminated composite beams", *Comput. Concr.*, **22**(6), 501-514. https://doi.org/10.12989/cac.2018.22.6.501

Lam K.Y. and Loy, C.T. (1994), "On vibration of thin rotating laminated composite cylindrical shells", *J. Sound Vib.*, **116**, 198. https://doi.org/10.1016/0961-9526(95)91289-S

Lee, S.Y., Huynh, T.C., Dang, N.L. and Kim, J.T. (2019), "Vibration characteristics of caisson breakwater for various waves, sea levels, and foundations", *Smart Struct. Syst.*, **24**(4), 525-539. https://doi.org/10.12989/sss.2019.24.4.525.

Li, H. and Lam, K.Y. (1998), "Frequency characteristics of a thin rotating cylindrical shell using the generalized differential quadrature method", *Int. J. Mech. Sci.*, **40**(5), 443-459. https://doi.org/10.1016/S0020-7403(97)00057-X

Li, H., Lu, H. and Li, Q. (2024), "Numerical investigations of the influences of valve spool structure on the eccentric jet flow characteristic in high-pressure angle valves", *Energy*, **298**, 131378. https://doi.org/10.1016/j.energy.2024.131378

Li, M., Wang, T., Chu, F., Han, Q., Qin, Z. and Zuo, M.J. (2021), "Scaling-basis chirplet transform", *IEEE T Ind. Electron.*, **68**(9), 8777-8788. https://doi.org/10.1109/TIE.2020.3013537

Liu, K., Zong, S., Li, Y., Wang, Z., Hu, Z. and Wang, Z. (2022), "Structural response of the U-type corrugated core sandwich panel used in ship structures under the lateral quasi-static compression load", *Marine Struct.*, **84**, 103198. https://doi.org/10.1016/j.marstruc.2022.10319

Loghman, A., Arani, A.G. and Barzoki, A.A.M. (2017), "Nonlinear stability of non-axisymmetric functionally graded reinforced nano composite microplates", *Comput. Concr.*, **19**(6), 677-687. https://doi.org/10.12989/cac.2017.19.6.677

Love, A.E.H. (1888), "The small free vibrations and deformation of thin elastic shell", *Phil. Trans. R. Soc. London*, **A179**, 491-549. https://doi.org/10.1098/rsta.1888.0016.

Loy, C.T., Lam, K.Y. and Shu, C. (1997), "Analysis of cylindrical shells using generalized differential quadrature", *Shock Vib.*, **4**, 193-198. https://doi.org/10.3233/SAV-1997-4305

Miaofen, L., Youmin, L., Tianyang, W., Fulei, C. and Zhike, P. (2023), "Adaptive synchronous demodulation transform with application to analyzing multicomponent signals for machinery fault diagnostics", *Mech. Syst. Signal Proc.*, **191**, 110208. https://doi.org/10.1016/j.ymssp.2023.110208

Mousavi, M., Mohammadimehr, M. and Rostami, R. (2019), "Analytical solution for buckling analysis of micro sandwich hollow circular plate", *Comput. Concr.*, **24**(3), 185-192. https://doi.org/10.12989/cac.2019.24.3.185

Muzamal, H. (2022), "Structural stability of laminated composite material for the effectiveness of half axial wave mode: frequency impact", *Adv. Concr. Constr.*, **14**(5), 309-315. https://doi.org/10.12989/acc.2022.14.5.309

Naeem, M.N. and Sharma, C.B. (2000), "Prediction of natural frequencies for thin circular cylindrical shells", *Proceedings of the Institution of Mechanical Engineers, Part C: Journal of Mechanical Engineering Science*, **214**(10), 1313-1328. https://doi.org/10.1243/0954406001523290

Najafizadeh, M.M. and Isvandzibaei, M.R. (2007), "Vibration of (FGM) cylindrical shells based on higher order shear deformation plate theory with ring support", *Acta Mechanica*, **191**, 75-91. http/10.1007/s00707-006-0438-0

Padovan, J. (1975), "Travelling waves vibrations and buckling of rotating anisotropic shells of revolution by finite element", *Int. J. Solid Struct.*, **11**(12), 1367-1380. https://doi.org/10.1016/0020-7683(75)90064-5

Penzes, R.L.E. and Kraus H. (1972), "Free vibrations of pre-stresses cylindrical shells having arbitrary homogeneous boundary conditions", *AIAA Journal*, **10**, 1309. https://doi.org/10.2514/3.6605

Poplawski, B., Mikulowski, G., Pisarski, D., Wiszowaty, R. and Jankowski, L. (2019), "Optimum actuator placement for damping of vibrations using the Prestress-Accumulation Release control approach", *Smart Struct. Syst.*, **24**(1), 27-35. https://doi.org/10.12989/sss.2019.24.1.027

Qazaq, A., Hussain, M., Mujalli, M. and Tounsi, A. (2022), "Fundamental computer assessment of ring support with exponent of trigonometric function: Safety geometrical perfection", *Adv. Concr. Constr.*, **14**(6), 381. https://doi.org/10.12989/acc.2022.14.6.381

Qin, C., Huang, G., Yu, H., Zhang, Z., Tao, J. and Liu, C. (2024b), "Adaptive VMD and multi-stage stabilized transformer-based long-distance forecasting for multiple shield machine tunneling parameters", *Automat. Constr.*, **165**, 105563. https://doi.org/10.1016/j.autcon.2024.105563

Qin, C., Shi, G., Tao, J., Yu, H., Jin, Y., Xiao, D. and Liu, C. (2024a), "RCLSTMNet: A residual-convolutional-LSTM neural network for forecasting cutterhead torque in shield machine", *Int. J. Control Auto Syst.*, **22**(2), 705-721. https://doi.org/10.1007/s12555-022-0104-x

Safaei, B., Khoda, F.H. and Fattahi, A.M. (2019), "Non-classical plate model for single-layered graphene sheet for axial buckling", *Adv Nano Res*, **7**(4), 265-275.

https://doi.org/10.12989/anr.2019.7.4.265
Saito, T. and Endo, M. (1986), "Vibrations of finite length rotating cylindrical shell", *J. Sound Vib.*, **107**, 17. https://doi.org/10.1016/0022-460X(86)90279-8
Sayin, E. and Calayir, Y. (2015), "Comparison of linear and non-linear earthquake response of masonry walls", *Comput. Concr.*, **16**(1), 17-35. https://doi.org/10.12989/cac.2015.16.1.017
Sewall, J.L. and Naumann, E.C. (1968), "An experimental and analytical vibration study of thin cylindrical shells with and without longitudinal stiffeners", *National Aeronautic and Space Administration, for sale by the Clearinghouse for Federal Scientific and Technical Information*, Springfield, Va, U.S.A.
Shahsavari, D., Karami, B. and Janghorban, M. (2019), "Size-dependent vibration analysis of laminated composite plates", *Adv. Nano Res.*, **7**(5), 337-349. https://doi.org/10.12989/anr.2019.7.5.337
Sharma, P., Singh, R. and Hussain, H. (2019), "On modal analysis of axially functionally graded material beam under hygro-thermal effect", *Proceedings of the Institution of Mechanical Engineers, Part C: Journal of Mechanical Engineering Science*, **234**(5), 1085-1101. https://doi.org/10.1177/0954406219888234.
Shi, J., Zhao, B., He, J. and Lu, X. (2024), "The optimization design for the journal-thrust couple bearing surface texture based on particle swarm algorithm", *Tribol. Int.*, **198**, 109874. https://doi.org/10.1016/j.triboint.2024.109874
Sivadas, K.R. and Ganesan, N. (1964), "Effect of rotation on vibrations of moderately thin cylindrical shell", *J. Vib. Acoust.*, **116**(1), 198-202 (1994). https://doi.org/10.1115/1.2930412
Srinivasan, A. V and Luaterbach, G.F. (1971), "Travelling waves in rotating cylindrical shells", *Trans. ASME, J. Eng. Ind.*, **93**, 1229-1232. https://doi.org/10.1115/1.3428067
Sun, R., Wang, S., Li, M. and Zhu, Y. (2025), "An algorithm for large-span flexible bridge pose estimation and multi-keypoint vibration displacement measurement", *Measurement*, **240**, 115582. https://doi.org/10.1016/j.measurement.2024.115582
Suresh, S. and Mortensen, A. (1997), "Functionally gradient metals and metal ceramic composites", *Part 2: Therm. Mech. Behav. Int. Mater.*, **42**, 85-116. https://doi.org/10.1179/imr.1997.42.3.85
Swaddiwudhipong. S, Tian. J. and Wang C.M. (1995), "Vibration of cylindrical shells with ring supports", *J Sound Vib.*, **187**(1), 69-93. https://doi.org/10.1006/jsvi.1995.0503
Tohidi, H., Hosseini-Hashemi, S.H. and Maghsoudpour, A. (2018), "Size-dependent forced vibration response of embedded micro cylindrical shells reinforced with agglomerated CNTs using strain gradient theory", *Smart Struct. Syst.*, **22**(5), 527-546. https://doi.org/10.12989/sss.2018.22.5.527
Toulokian Y.S. (1967), *Thermo Physical Properties of High Temperature Solid Materials*, Macmillan, New York, U.S.A.
Wang, S., He, J., Fan, J., Sun, P. and Wang, D. (2023), "A time-domain method for free vibration responses of an equivalent viscous damped system based on a complex damping model", *J. Low Freq. Noise Vib. Active Control*, **42**(3), 1531-1540. https://doi.org/10.1177/14613484231157514
Wang, T., Liang, M., Li, J. and Cheng, W. (2014), "Rolling element bearing fault diagnosis via fault characteristic order (FCO) analysis", *Mech. Syst. Signal Pr.*, **45**(1), 139-153. https://doi.org/10.1016/j.ymssp.2013.11.011
Xiang, (2012), "Natural frequencies of rotating functionally graded cylindrical shells", *Appl. Math. Mech. Engl. Ed.*, **33**(3), 345-356. https://doi.org/10.1007/s10483-012-1554-6
Yeh, J.Y. (2016), "Vibration characteristic analysis of sandwich cylindrical shells with MR elastomer", *Smart Struct. Syst.*, **18**(2), 233-247. https://doi.org/10.12989/sss.2016.18.2.233
Yuan, X., Wang, W., Pang, H. and Zhang, L. (2024), "Analysis of vibration characteristics of electro-hydraulic driven 3-UPS/S parallel stabilization platform", *Chinese J. Mech. Eng.*, **37**(1), 96. https://doi.org/10.1186/s10033-024-01074-w
Zahrai, S.M. and Kakouei, S. (2019), "Shaking table tests on a SDOF structure with cylindrical and rectangular TLDs having rotatable baffles", *Smart Struct. Syst.*, **24**(3), 391-401. https://doi.org/10.12989/sss.2019.24.3.391
Zhang, S., Liu, L., Zhang, X., Zhou, Y. and Yang, Q. (2024), "Active vibration control for ship pipeline system based on PI-LQR state feedback", *Ocean Eng.*, **310**, 118559. https://doi.org/10.1016/j.oceaneng.2024.118559
Zhang, Z. and Ma, X. (2024), "Friction-induced nonlinear dynamics in a spline-rotor system: Numerical and experimental studies", *Int. J. Mech. Sci.*, **278**, 109427. https://doi.org/10.1016/j.ijmecsci.2024.109427
Zheng, Y., Chu, L., Dui, G. and Zhu, X. (2021), "Modeling and simulation of functionally graded flexoelectric micro-cylinders based on the mixed finite element method", *Appl. Phys. A*, **127**, 1-16. https://doi.org/10.1007/s00339-021-04316-z
Zohar, A. and Aboudi, J. (1973), "The free vibrations of thin circular finite rotating cylinder", *Int. J. Mech. Sci.*, **15**, 269-278. https://doi.org/10.1016/0020-7403(73)90009-X.

CC

Appendix

Where

$$\bar{m}_{11}= A_{11}\frac{\partial^2}{\partial x^2}+\left(\frac{A_{66}}{R^2}+\rho_t \pounds^2\frac{\partial^2}{\partial\theta^2}\right).$$

$$\bar{m}_{12}= \frac{(A_{12}+A_{66})}{R}\frac{\partial^2}{\partial x\partial\theta}+\frac{(B_{12}+2B_{66})}{R^2}\frac{\partial^2}{\partial x\partial\theta}$$

$$\bar{m}_{13}= \left(\frac{A_{12}}{R}-\rho_t \pounds^2 R\right)\frac{\partial}{\partial x}-B_{11}\frac{\partial^3}{\partial x^3}-\frac{(B_{12}+2B_{66})}{R^2}\frac{\partial^3}{\partial x\partial\theta^2}$$

$$\bar{m}_{21}= \left(\frac{A_{12}+A_{66}}{R}+\frac{B_{12}+B_{66}}{R^2}+\rho_t \pounds^2 R\right)\frac{\partial^2}{\partial x\partial\theta}$$

$$\bar{m}_{22}= \left(A_{66}+\frac{3B_{66}}{R}+\frac{2D_{66}}{R^2}\right)\frac{\partial^2}{\partial x^2}$$
$$+\left(\frac{A_{22}}{R^2}+\frac{2B_{22}}{R^3}+\frac{D_{22}}{R^4}\right)\frac{\partial^2}{\partial\theta^2}+\rho_t \pounds^2$$

$$\bar{m}_{23}= \left(\frac{A_{22}}{R^2}+\frac{B_{22}}{R^3}\right)\frac{\partial}{\partial\theta}-\left(\frac{B_{22}}{R^3}+\frac{D_{22}}{R^4}\right)\frac{\partial^3}{\partial\theta^3}$$
$$-\left(\frac{B_{12}+2B_{66}}{R}+\frac{D_{12}+2D_{66}}{R^2}\right)\frac{\partial^3}{\partial x^2\partial\theta}-2\rho_t \pounds\frac{\partial}{\partial t}$$

$$\bar{m}_{31}= -\frac{A_{12}}{R}\frac{\partial}{\partial x}+B_{11}\frac{\partial^3}{\partial x^3}+\left(\frac{B_{12}+2B_{66}}{R^2}\right)\frac{\partial^3}{\partial x\partial\theta^2}$$

$$\bar{m}_{32}= -\left(\frac{A_{22}}{R^2}+\frac{B_{22}}{R^3}+\rho_t \pounds^2\right)\frac{\partial}{\partial\theta}+\left(\frac{B_{22}}{R^3}+\frac{D_{22}}{R^4}\right)\frac{\partial^3}{\partial\theta^3}$$
$$+\left(\frac{B_{12}+2B_{66}}{R}+\frac{D_{12}+4D_{66}}{R^2}\right)\frac{\partial^3}{\partial x^2\partial\theta}+2\rho_t \pounds\frac{\partial}{\partial t}$$

$$\bar{m}_{33}= -\frac{A_{22}}{R^2}+\rho_t \pounds^2+\frac{2B_{12}}{R}\frac{\partial^2}{\partial x^2}+\left(\frac{2B_{22}}{R^3}+\rho_t \pounds^2\right)\frac{\partial^2}{\partial\theta^2}$$
$$-D_{11}\frac{\partial^4}{\partial x^4}-2\left(\frac{D_{12}+2D_{66}}{R^2}\right)\frac{\partial^4}{\partial x^2\partial\theta^2}-\frac{D_{22}}{R^4}\frac{\partial^4}{\partial\theta^4}$$